Large 10-dB Bandwidth and Low Insertion Loss Silicon Dual-ring Modulator

Hongxia Zhang
Department of Electronic Engineering
Shanghai Jiao Tong University
Shanghai, China
zhanghongxia@sjtu.edu.cn

Xinhong Jiang
Department of Electronic Engineering
Shanghai Jiao Tong University
Shanghai, China
jiangxinhong@sjtu.edu.cn

Ciyuan Qiu*
Department of Electronic Engineering,
Shanghai Jiao Tong University
Shanghai, China
*qiuciyuan@sjtu.edu.cn

***Abstract*—A silicon dual-ring modulator with 10-dB bandwidth of 0.08 nm and low insertion loss of 1.1 dB is experimentally demonstrated. The modulation speed of the dual-ring modulator can be as high as 20 Gb/s.**

Keywords—dual-ring modulator, large bandwidth, low insertion loss

I. INTRODUCTION

Silicon electro-optic (EO) modulators are the basic and fundamental components for silicon based integrated optical transmission systems [1]. Several types of on-chip silicon modulators have been realized by Mach-Zehnder interferometers (MZIs) [2], microring resonators (MRRs) [3], etc. Among these demonstrated silicon modulators, silicon microring modulators attract much attention owing to its compact footprint and low power consumption [4]. To achieve high signal-to-noise ratio (SNR), lower insertion loss and large modulation depth are needed. However, the resonance wavelength of a microring modulator is highly susceptible to fabrication variations and temperature fluctuations, which will influence the insertion loss and the modulation depth. Thus the SNR of the modulated optical signal will be deteriorated.

To date, various schemes have been used to address this issue, such as wavelength locking and increasing the bandwidth of the microring modulators. Wavelength locking needs to monitor the optical power and adjust the heating power based on the monitored optical signal [5]. Monitoring signals can be obtained from the through or drop ports, which increases the insertion loss of the modulator. Furthermore, it is still hard to precisely control the heating power, and resonance wavelength mislignment may still exist, which will deteriorate the SNR. By increasing the bandwidth of microring modulators, the influence of resonance wavelength drift can be decreased. To enlarge the bandwidth of a microring modulator, a modulator consists of two cascaded microring resonators has been experimentally demonstrated in [6]. A 10-dB bandwidth of ~0.07 nm is obtained. However, since the resonance wavelengths for the cascaded microring simultaneously blue shift or red shift, its modulation efficiency is close to that of a single microring modulator. To achieve a moderate resonance shift and large modulation depth, a large insertion loss of 4.4 dB is introduced. A silicon dual-ring modulator is proposed in [7]. Thanks to the push-pull configuration, large 10-dB bandwidth and low insertion loss can be obtained with low power consumption. However, this device has not been experimentally demonstrated.

In this paper, we experimentally demonstrate the EO push-pull dual-ring modulator. The 10-dB bandwidth of the dual-ring modulator is 0.08 nm and the insertion loss is 1.1 dB. The bandwidth is wider and insertion loss is lower than a single microring modulator when the modulation depth is about 10 dB, benefiting from the electromagnetically induced transparency (EIT)-like effect and push-pull configuration [7-8].

II. DEVICE STRUCTURE AND OPERATION PRINCIPLE

Fig. 1(a) shows the structure of the proposed dual-ring modulator. The black lines represent the silicon optical waveguides. The cross-section of the waveguide is shown in Fig. 1(b). The radius R of ring 1 and ring 2 are 12.5 μm. The distance between the centers of the two rings is πR. Thus, electromagnetically induced transpatency (EIT)-like effect can be obtained [8] and the insertion loss is reduced. The blue and yellow regions represent highly doped p++ and n++ regions, respectively. The light-blue and light-yellow regions represent slightly doped p+ and n+ regions, respectively. The highly doped concentration are 2.27×10^{17} cm^{-3} and 1.12×10^{17} cm^{-3} for p++ and n++ in the fabrication, respectively. The red annular region above the two rings represent micro-heaters, which are designed to compensate fabrication errors and temperature variations, as well as setting the initial resonance wavelength offset of the two microring resonators by heating the resonators. The equivalent electrical circuit of the dual-ring modulator is depicted in Fig. 1(c). The two p-n junctions of the two rings are back to back. R_i denotes the contact resistance of the metal wires and the doped silicon areas. R_t is the characteristic impedance which is optimized to approach 50 Ohm to achieve a fast modulation.

The dual-ring modulator was fabricated on a silicon-on-insulator (SOI) wafer in the Institute of Microelectronics (IME) in Singapore. Fig. 1(d) shows the micrograph of the fabricated modulator. The silicon waveguide is 500 nm wide and 220 nm high with a slab thickness of 60 nm. All the highly doped n++ regions are electrically connected by metal wires. The left two lateral TO lines are metal wires that connect the integrated micro-heater for the ring 1. The right two lateral TO lines are metal wires that connect the integrated micro-heater for the ring 2. By applying electrical power on the two micro-heaters, the detuning of the two rings can be adjusted through the thermo-optic effect of silicon. The three vertical EO lines are metal wires that connect the highly doped areas. Then, the electro-optic modulation voltage V_1 and V_2 can be applied to the dual-ring modulator.

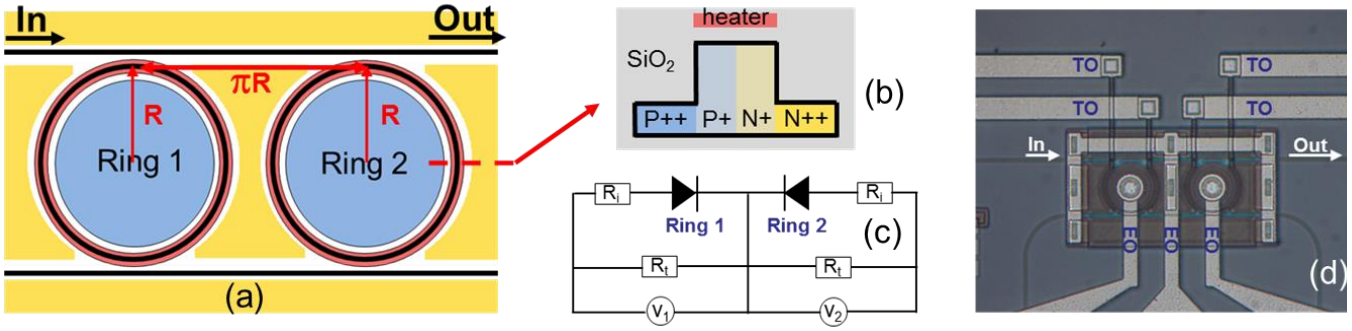

Fig. 1 (a) Schematic diagram of the dual-ring modulator. (b) Cross-section view of the dual-ring modulator. (c) Equivalent circuit of the dual-ring modulator. (d) Micrograph of the fabricated dual-ring modulator.

III. Experimental Results and Disscussions

The transmission spectra in the static EO modulation is firstly measured after removing the impedance resistance R_t. Fig. 2(a) shows the normalized transmission spectra of EO modulation of ring 1. When the applied voltage is reverse biased, the resonance wavelength blue shifts due to free carrier dispersion effect. From forward bias 0.5 V to reverse bias 5 V, the resonance wavelength of ring 1 shifts 80 pm. The 10-dB bandwidth of ring 1 is 0.03 nm and the lowest insertion loss is 2.69 dB. Fig. 2(b) shows the resonance shift of ring 1 versus the reverse bias voltage with a slope of ~11 pm/V. Fig. 2(c) shows the normalized transmission spectra of EO modulation of ring 2. From forward 0.5 V to reverse 5 V, the resonance of ring 2 shifts 72 pm. The 10-dB bandwidth of ring 2 is 0.02 nm and the lowest insertion loss is 4.1 dB. Fig. 2(d) shows the resonance shift of ring 2 versus the reverse bias voltage, the slope is also about 11 pm/V. Fig. 2(e) and 2(f) show the normalized transmission of the dual-ring with different voltages. When the applied voltage of ring 1 is reverse bias 5 V, the resonance wavelength of ring 1 blue shifts. Meanwhile, the applied voltage of ring 2 is forward bias 0.5 V, the resonance wavelength of ring 2 red shifts. Then the resonance of the dual-ring modulator can be aligned. When the applied voltage of ring 1 is forward bias 0.5 V and the applied voltage of ring 2 is reverse bias 5 V, the detuning of the two rings will increase. The 10-dB bandwidth of the dual-ring modulator is 0.07 nm and the lowest insertion loss is 2.19 dB. When the reverse bias increases to 7 V, the 10-dB bandwidth of the dual-ring modulator is 0.08 nm and the lowest insertion loss is 1.1 dB. The dual-ring modulator can achieve a better performance when the applied reverse bias is large.

Then the eye diagrams of Ring 1 and Ring 2 are measured

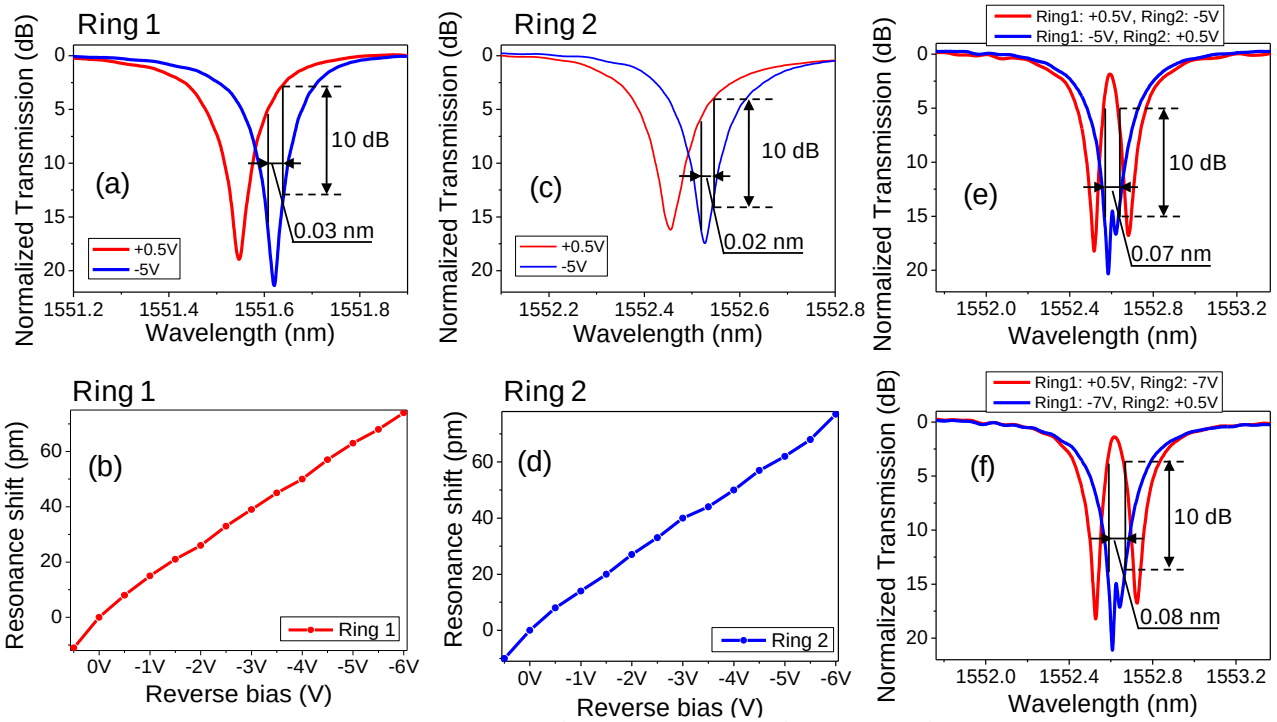

Fig. 2 Normalized transmission spectra and resonant wavelength shift versus the reverse bias of ring 1 (a), (b), of ring 2 (c), (d). Normalized transmission spectra of dual-ring with different voltages: (e) Vpp: 5.5 V, (f) Vpp: 7.5 V.

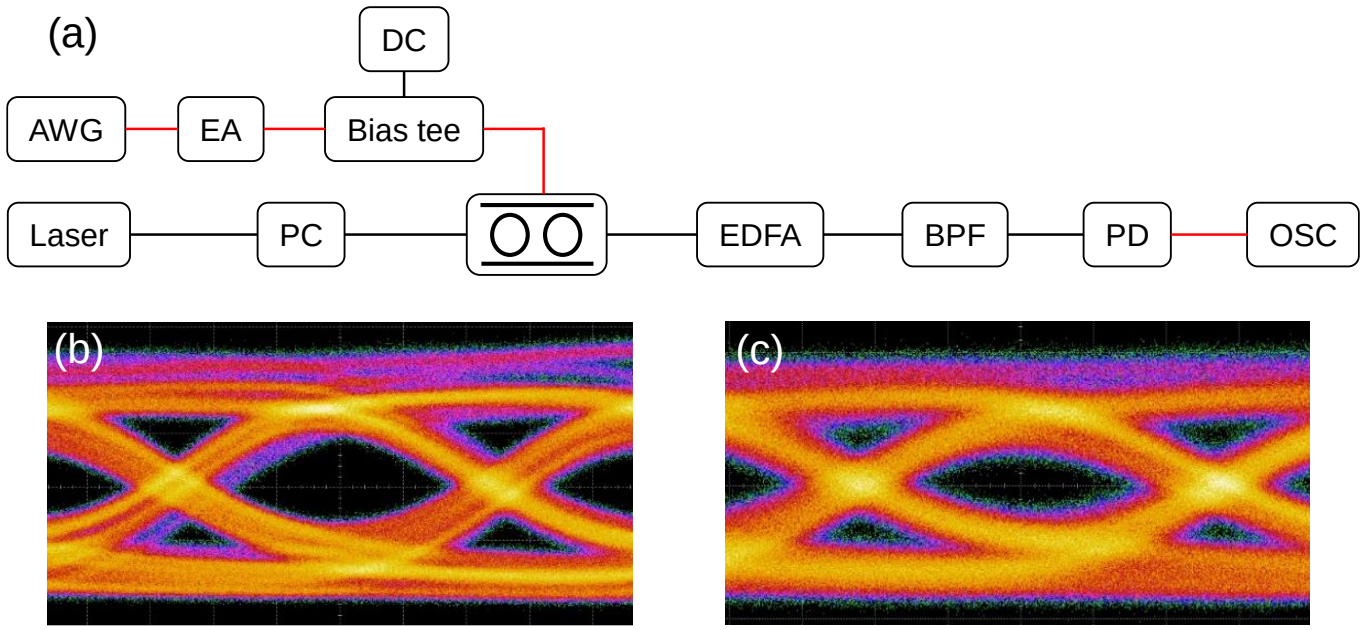

Fig. 3 (a) Experimental setup for testing eye diagrams. The red lines represent electrical signals. The black lines represent optical signals. (b) 20 Gb/s eye diagram of ring 1. (c) 20 Gb/s eye diagram of ring 2.

separately to verify the modulation speed. The experimental setup is shown in Fig. 3(a). The pseudo-random bit sequence (PRBS) data signal, generated by an arbitrary waveform generator (AWG), is amplified by a electricity amplifier (EA) and the V_{pp} for the amplified signal is 5.5 V. Then the amplified electrical signal is biased at -2.25V and thus the voltage of the signal ranges from forward 0.5 V to reverse 5 V, which is used to drive the modulator through a radio-frequency (RF) probe. The operation wavelength and the output power of the laser are set to be resonance wavelength and 6 dBm, respectively. The optical power is then attenuated to −1 dBm before injected to the dual-ring modulator to get rid of the thermal effect. The polarization of light beam is controlled by the polarization controller (PCs) to be quasi-TE. After the dual-ring modulator, the signal is amplified using Erbium-doped fiber amplifiers (EDFA). Then a band pass filter (BPF) is employed to suppress amplified spontaneous emission (ASE) noise. The optical signal is then converted to the electrical signal by a high speed photodetector (PD) and fed to the oscilloscope (OSC) for detection. Edge coupling is used to couple light between optical fibers and silicon waveguides. The coupling loss is about 5 dB/facet. As shown in Fig. 3(b) and 3(c), the eye diagrams of ring 1 and ring 2 are obtained with a speed about 20 Gb/s.

IV. Summary

We experimentally demonstrated a push-pull silicon dual-ring modulator with a 10-dB bandwidth of 0.08 nm and a low insertion loss of 1.1 dB. The static experimental spectra indicates that the dual-ring modulator has a better performance than the single microring modulator. The modulation speed of the device is verified to be as high as 20 Gb/s. The next step is to test the eye diagrams of the dual ring modulator.

References

[1] G. Reed, G. Mashanovich, F. Gardes, and D. Thomson, “Silicon optical modulator,” Nature Photonics, vol 4, pp. 518-526, August 2010.

[2] P. Dong, L. Chen, Y. Chen, “High-speed low voltage single-drive push-pull silicon Mach-Zehnder modulators”, Optics Express, vol. 20, pp. 6163-6169, February 2012.

[3] W. Bogaerts, P. Heyn, T. Vaerenbergh, K. Vos, S. Selvaraja, T. Clases and et al. “Silicon microring resonators”, Laser Photonics Reviews 6, No. 1, pp. 47-73, 2012.

[4] J. Rosenberg, W. Green, D. Gill, T. Barwicz, M. Shank, and Y. Vlasov, “A 25 Gbps silicon microring modulator based on an interleaved junction”, Optics Express, vol 20, pp. 26411-26423, November 2012.

[5] A. Melikyan, K. Kim, Y. Chen, P. Dong, “Tapless Locking of Silicon Ring Modulators for WDM Applications,” in Optical Fiber Communication Conference 2017, p. Tu2H.6.

[6] Y. Hu, X. Xiao, H. Xu, X. Li, K. Xiong, Z. Li, T. Chu, Y. Yu, and J. Yu, “High-speed silicon modulator based on cascaded microring resonators,” Optics Express, vol. 20, pp. 15079-15085, July 2012.

[7] Q. Xu, “Silicon dual-ring modulators,” Optics Express, vol 17, pp. 20783-20793, November 2009.

[8] Q. Xu, S. Sandhu, M. L. Povinelli, J. Shakya, S. Fan, and M. Lipson, “Experimental realization of an on-chip all-optical analogue to electromagnetically induced transparency”, Physical Review Letters, vol. 96, pp. 12-31, March 2006.